LeTID Mitigation via an Adapted Firing Process in p-Type PERC Cells from SMART Cast-Monocrystalline, Czochralski and High-Performance Multicrystalline Silicon

Felix Maischner[1], Stephan Maus[1], Johannes Greulich[1], Sabrina Lohmüller[1], Elmar Lohmüller[1], Pierre Saint-Cast[1], Daniel Ourinson[1], Henri Vahlman[1], Karin Hergert[2], Stephan Riepe[1], Stefan Glunz[1], Stefan Rein[1]

[1]Fraunhofer Institute for Solar Energy Systems ISE, Freiburg, Germany [2]Rehm Thermal Systems GmbH, Blaubeuren, Germany

Abstract

In this work, we analyse passivated emitter and rear cells (PERC), based on wafers made from seed manipulation for artificially controlled defects technique (SMART) monocrystalline silicon, magnetically-grown and conventional Czochralski (mCz and Cz) silicon, and high-performance multicrystalline (hpm) silicon. All wafers were processed identically except for the hpm wafers, which received an acidic texture instead of random pyramids. The energy conversion efficiency η of the SMART cells of 21.4 % is similar to the mCz cells (21.5 %) while being more than 1.9 $\%_{abs}$ higher than for the hpm cells. Furthermore, we here show for the first time that light and elevated temperature induced degradation (LeTID) is mitigated in hpm, Cz and SMART PERC cells without significant losses in initial efficiency by an adapted fast firing process, incorporating slower firing ramps that can be used in industrial production. The cells that are fired with these ramps show no significant efficiency loss ($1\,\%_{rel} < \Delta\eta < 2\,\%_{rel}$) during LeTID testing at 75 °C and 0.15 suns illumination for 1100 hours, while the reference fast firing process results in efficiency losses of $5\,\%_{rel} < \Delta\eta < 6\,\%_{rel}$ due to LeTID. For Cz cells that have been treated to regenerate the boron-oxygen defect prior to LeTID testing, the maximum degradation was reduced from $\Delta\eta \approx 3\,\%_{rel}$ to $\Delta\eta \approx 1.5\,\%_{rel}$.

1 Introduction

Seed manipulation for artificially controlled defects technique (SMART) is a crystallization technique which is based on the vertical gradient freeze (VGF) technique and allows monocrystalline silicon ingots and wafers to be grown which are virtually free of dislocations, grain boundaries and parasitic multicrystalline grains [1] opposed to conventional mono-cast wafers. This is achieved by introducing functional defects on the edges of each ingot in addition to monocrystalline seed plates to reduce stress and prevent grains originating at the crucible wall from growing inward during the crystallization process. The method therefore combines the low production cost and low oxygen contamination of high-performance multicrystalline (hpm) silicon wafers with the superior optical properties of Czochralski (Cz) silicon solar cells, due to the possibility of using alkaline texturing. It has been recently shown that the SMART approach works on a small scale [2] as well as on G2 ingots [3].

Light and elevated temperature induced degradation (LeTID) [4] is a defect mechanism that especially affects passivated emitter and rear cells (PERC) [5]. It is known to reduce the cell energy conversion efficiency η by up to 10 $\%_{rel}$ and more [6]. Since wafers grown by the VGF technique contain little oxygen and thus show little boron-oxygen (BO) related light-induced degradation (BO-LID), LeTID is typically the dominating degradation effect. The exact defect which is causing LeTID is still unknown and there are different models to describe it [7, 8, 9, 10]. However, all cited models agreed that hydrogen plays some role in the defect formation. For a more in depth analysis of the LeTID defect, the different models and possible mitigation methods, I recommend reading the review paper by Chen *et al.* [11].

It is known that high temperature processing steps can determine the existence and extent of LeTID. It can for example be eliminated by reducing the peak temperature in the fast firing step of the cell production [12, 13], but these results were only shown on lifetime samples. When facing the challenge of forming a contact with low contact resistance, this approach has detrimental effects on the cell performance [14]. The only study using this method on cells did not report the initial efficiencies that were achieved [15]. However, they did publish the poweroutput of modules that were fabricated with these cells. The module performance was about the same of a module made out of aluminum backsurface field (Al-BSF) cells. Since PERC cells usually far outperform Al-BSF cells, it is likely that the initial efficiencies of the cells suffered from their process.

Other approaches include adding an additional annealing step after the first firing [13], or annealing prior to firing [16]. During the annealing the samples are illuminated to create excess carriers. These methods would complicate cell production since further processing steps are necessary. Additionally, these processes have been shown to lead to overfiring and with it to increased series resistance and reduced shunt resistance [13] or increased surface recombination [16].

Moreover, it has been suggested that using slower cooling ramps in this process might reduce or eliminate LeTID [17]. Even though no results were published to back this claim, the idea inspired further research. So far, it has been shown that greatly reducing the cooling rate or slowing down the whole firing process by lowering the belt speed reduces LeTID in hpm lifetime samples [18, 19]. Only reducing the slope of the cooling ramp has been shown to work on lifetime samples out of conventional mono-cast material, when reducing the cooling rate to 20 K/s [20] or even up to 50 K/s in p-type Cz lifetime samples [21]. All these analyses have been done without addressing the challenges of realizing these processes on equipment suited for industrial production and without negatively impacting surface passivation and contact formation and hence energy conversion efficiency compared to conventional firing processes.

In this work, we compare essentially identically processed hpm, SMART and magnetically-grown Czochralski (mCz) silicon cells and show that SMART wafers can be used to produce cells with efficiencies similar to mCz cells, far outperforming standard hpm. Moreover, we introduce a fast firing process with a slower cooling ramp, compared to a standard firing process. We established this process on an industrial fast firing oven (FFO) and show that it mitigates LeTID in cells while still achieving as high efficiencies as with the standard reference process. The tool is fully industrially feasible and the cycle time is not increased compared to the reference process. No additional processing steps before of after firing are needed.

2 Experimental

2.1 Solar Cell Production

We fabricated a batch of boron-doped p-type silicon PERC cells out of two SMART centre bricks from different G2 ingots. We took full square wafers with an edge length of 156.6 mm out of the centre region of these bricks called SMART 1 and SMART 2; the base resistivities are 0.8 Ωcm and 1.4 Ωcm, respectively. To be able to investigate the impact of the grain boundaries formed at the transitions between seed plates, the bricks were cut from the ingots in a way that two of these seed-related grain boundaries run through the wafers as can be seen in the photoluminescence (PL) image in Figure 2. As a reference, we also processed boron-doped mCz and hpm wafers with base resistivities of 0.8 Ωcm and 1.5 Ωcm and wafer sizes of M0 and 156.3 mm full square, respectively.

The hpm wafers received an acidic texture, whereas the SMART and mCz wafers were alkaline textured using KOH. Other than that, all wafers were processed identically and at the same time. The emitter was formed using a $POCl_3$ diffusion. Afterwards, they received a single side emitter removal and a phosphosilicate glass etch. The rear side was passivated with 6 nm atomic layer deposited Al_2O_3. After an outgassing step, the Al_2O_3 was capped with 150 nm of SiN_x using plasma-enhanced chemical vapour deposition (PECVD). The front side was passivated with 75 nm of SiN_x also using PECVD. The rear side was locally opened using laser contact opening (LCO). The LCO was done on all samples with dots of 19 μm radius, but the pitch was adapted for samples of different base resistivity (450 μm for the higher doped mCz and SMART 1 cells and 350 μm for the lower doped hpm and SMART 2 cells).

All cells were screen-printed with the same commercially available pastes using a five busbar monofacial layout with 110 fingers and a finger width of 33 μm. The SMART cells were printed with the same screen as the hpm cells, even though the SMART cells are slightly larger. Due to their pseudo-square shape, the contacts on the mCz wafers were screen-printed with different metallization layouts.

To investigate the influence of the fast firing process on cell efficiency and LeTID mitigation, all but the mCz wafers were subdivided in six groups, and were fired in an FFO by the company Rehm Thermal Systems GmbH, Germany, using three different set peak temperatures (810 °C, 830 °C and 850 °C) each with two different cooling ramps. Figure 1 shows two of the investigated FFO profiles. To record these profiles, one cell of each group was fired while being attached to a frame. This allows for a thermocouple anchored at the frame to press against the centre of the cell by spring force, as can be seen in Figure 3a in this paper by Ourinson *et al.* [22]. The thermocouple has a wire connection to a data logger to record the measured data. The datalogger is placed into a thermal shield box for heat protection during the firing process. The slopes of the cooling ramps were calculated from the slope between two points. The first point is chosen one second after the peak temperature is reached to disregard the region where the slope is rapidly increasing. The second point is chosen at the time at which the temperature reaches 600 °C. The new slower cooling ramp was set to 50 K/s, whereas the standard ramps have a cooling slope of 60 K/s, 70 K/s or 72 K/s, depending on the peak temperature. The mCz wafers were all fired at 850 °C with a standard cooling ramp.

Alongside the cells, we also prepared samples from each material, which were prepared identically, only leaving out the LCO and screen printing. In the following text, we call these samples implied open-circuit voltage (iV_{OC}) samples. Moreover, additional samples are made on mCz wafers (1.3 Ωcm) with an acidic texture and on n-type Cz wafers

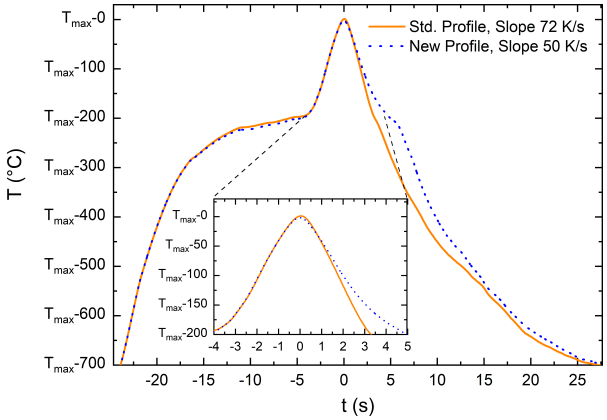

Figure 1: Time-temperature profiles of fast-firing processes with a set peak temperature of 850 °C and two different cooling rates. The inset shows a magnification of the data in the region around the peak.

(4.0 Ωcm) with an alkaline texture. These are here called emitter dark saturation current (J_{0e}) samples. From these samples the emitter was not removed from either side. Otherwise they were processed similarly to the iV_{OC} samples except for the surface passivation stack and the firing peak temperature. In the case of the J_{0e} samples, these were a symmetric stack of PECVD-deposited SiN_x (75 nm) and 820 °C, respectively.

In a second batch, cells were made out of boron-doped p-type Cz silicon with a base resistivity of 0.6 Ωcm using the same process sequence as above but with a rear SiN_x layer thickness of 80 nm.

2.2 LeTID Investigation

After firing all cells, they were analysed with an inline current-voltage (IV) tester. The most efficient cells of each material were given to Fraunhofer ISE CalLab PV Cells, to validate the results. The two median cells of each group were used for the LeTID investigation. The selected samples were BO-degraded for 48 hours at room temperature under 0.05 suns illumination under open-circuit conditions. Afterwards, they were tested for LeTID on a hotplate at 75 °C under an illumination intensity of 0.15 suns for 1100 hours, also under open-circuit conditions. These conditions were chosen to evaluate the degradation that a solar cell mounted on a German rooftop would undergo within a 20 year lifespan [23]. The illumination is chosen at 0.15 suns because the resulting excess carrier density at open-circuit conditions roughly resembles that of a cell at 1 sun illumination, operating at the maximum power point, as it has been suggested for testing [24]. During the degradation, the cells were taken off the hotplate regularly to measure IV-curves, reflectance and internal quantum efficiency (IQE) and to take electroluminescence (EL) images under standard test conditions. Care was taken to keep the cells in the dark between degradation steps and measurements.

Since Cz material contains significant amounts of oxygen, it is expected to show a strong BO-degradation. It has been shown, that the BO-defect also degrades and subsequently regenerates at the conditions we have chosen for LeTID testing [25]. If these cells would be LeTID tested directly after firing, this regeneration might mask the simultaneous LeTID degradation. One method to quickly regenerate the BO-defect are laser based processes[26, 27]. We regenerated the BO-defect in the cells of the second batch using the LID regeneration tool RRS-LID from Rehm Thermal Systems prior to the LeTID test [28]. The treatment was done for 8.5 s with an adapted laser intensity profile to ensure constant sample temperature of 270 °C during regeneration. After this treatment, some BO-defects are not in the regenerated but only in the annealed

state. To avoid the confusion of these defects with the LeTID defect, the cells have subsequently been BO-degraded identically to all other cells.

3 Results

3.1 Initial efficiencies

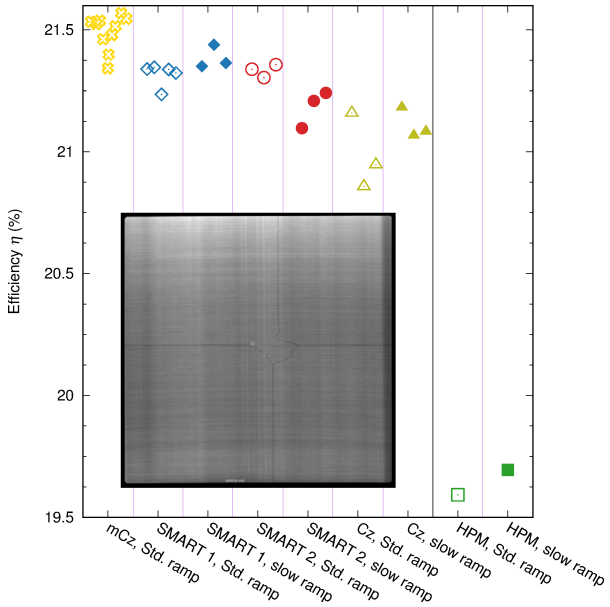

Figure 2: Efficiencies for different materials and FFO ramps after firing. Only the set peak temperature that achieved the highest η is shown. For Cz cells values were measured after BO-degradation. The bottom left corner shows a PL image of an as-cut SMART wafer with crossover of the seed-plate-related grain boundaries.

Figure 2 shows the efficiency as measured after firing (as-processed). Only the results of the set peak temperature that achieved the highest η are shown here (same for all groups). The most efficient cells per material were measured to have an efficiency of 21.5 % for mCz, 21.4 % for SMART, and 19.7 % for hpm, all measured by Fh-ISE CalLab. In a parallel solar cell batch an efficiency of up to 21.5 % was achieved using the SMART 1 brick we used in this study [29]. Later, the same material was used to achieve an even higher efficiency of up to 21.9 % mainly due to using a zero busbar layout [29]. The highest efficiency of a Cz cells was measured to be 21.2 %. However, the measurements of the Cz cells were taken after the BO-degradation and cannot be compared to those of the other cells because of different cell processing.
As can be seen in Figure 2, no significant difference in the as-processed efficiencies between standard firing (open symbols) and the adapted firing with a slower cooling ramp (closed symbols) can be observed before the LeTID stability test.

3.2 LeTID test

Figure 3 shows the results of the LeTID test in terms of relative degradation of η. After the BO-degradation, the efficiencies of all cells drop by 0.8%$_{rel}$ to 1.8%$_{rel}$. The cells fired with the slower cooling ramp are a little less affected by this degradation. Over the cause of the LeTID test, the hpm and SMART cells that were fired with the standard ramp show a strong degradation, with loss of up to 5.5 %$_{rel}$ in efficiency. The SMART cells subsequently regenerate to about their initial efficiency. The counterparts fired with the improved ramp show losses that are lower than

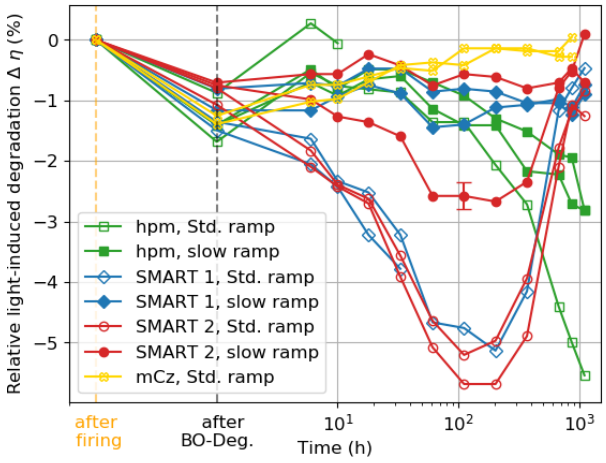

Figure 3: Relative change in η after BO-degradation and during the LeTID test under an illumination intensity of 0.15 suns at 75 °C in reference to the initial efficiency after firing of the two median cells of each group. To improve readability and since the error is assumed to be identical for each measurement, the error bar is only displayed for a single measurement.

1.5 %$_{rel}$ and 3 %$_{rel}$ for SMART and hpm, respectively, with the exception of one SMART 2 sample that degraded up to 2.8 %$_{rel}$. On the other hand, the mCz samples show no clear signs of LeTID. It is also apparent that the hpm cells did not reach the minimum of the degradation-regeneration cycle during the period of the degradation test. Also, it can be seen that the hpm cells show an increase in efficiency of about 1 %$_{rel}$ after the first minute of the LeTID test.
Figure 4 shows the relative change of open-circuit voltage V_{OC} and short-circuit current density J_{SC} during the LeTID test. Overall, the behaviour looks similar to the behaviour of η. The V_{OC} and J_{SC} of the SMART cells fired with the standard ramp both drop and recover around the same time during the test. However, the impact of J_{SC} on η is greater than the impact of V_{OC}. This can be seen by comparing the maximum relative degradation of 1.8-2.2 % in J_{SC} to the maximum relative degradation of 1.1-1.7 % in V_{OC}.
Comparing the two SMART materials fired with the standard ramp, it is apparent that the cells with the SMART 1 material degrade in V_{OC} more strongly. The same is true for J_{SC} but the effect is less pronounced. Within the error of the measurement it might also be true that there is no difference in J_{SC} at all between both material types.
The slowly fired SMART samples drop by up to only 0.5 %$_{rel}$ in V_{OC} and 1.0 %$_{rel}$ in J_{SC}. Only the hpm cells degrade in J_{SC} more than the SMART cells with a degradation continuing even at the end of the test.
Figure 5 shows the change of fill factor FF and pseudo fill factor pFF during the LeTID test. The drop in FF for the SMART 2 cells fired with the standard ramp cells is about 2.5 %$_{rel}$, compared to only 1.3 %$_{rel}$ for the SMART 1 cells. With the exception of one outlier, the SMART cells fired with a slower cooling ramp, as well as all Cz and hpm cells only degrade by up to 0.6 %$_{rel}$.
Comparing FF and pFF, both behave very similarly in the course of the LeTID test. It should be noted that the results of one hpm sample are not shown in the pFF plot. The initial pFF measurement was faulty, rendering an analysis of the relative change to that initial value useless.
Figure 6 shows the result of the LeTID test of the Cz cells fabricated in an separate experiment with the same process sequence as the cells discussed above but with a rear SiNx layer being almost 50% thinner. All samples show a loss in η. Analysing the amount of maximum degradation, a clear trend becomes apparent. The amount of degradation is lower in cells fired with the slower cooling ramp. The slower cooling reduced the maximum degradation from 3.3% to 1.5%.

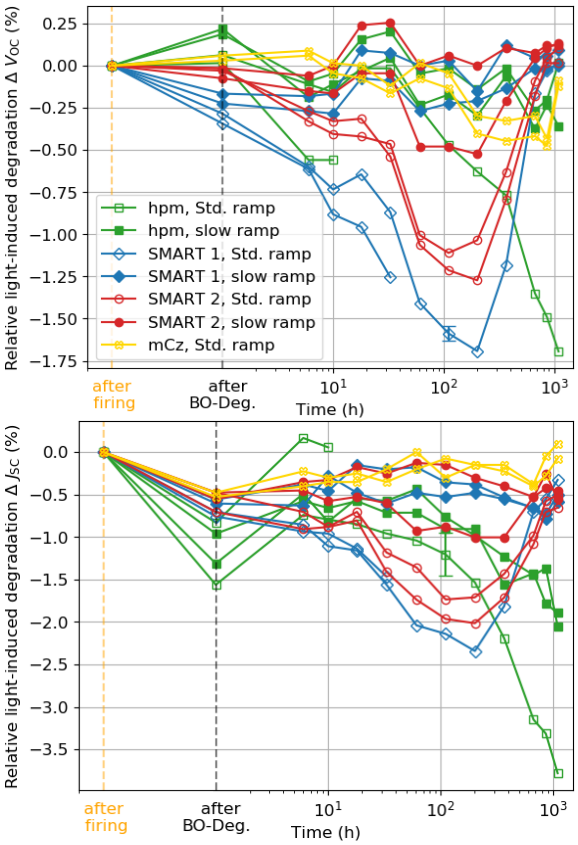

Figure 4: Relative change in V_{OC} and J_{SC} after BO-degradation and during the LeTID test under an illumination intensity of 0.15 suns at 75 °C in reference to the respective initial value after firing. The error bars are handled as in Figure 3.

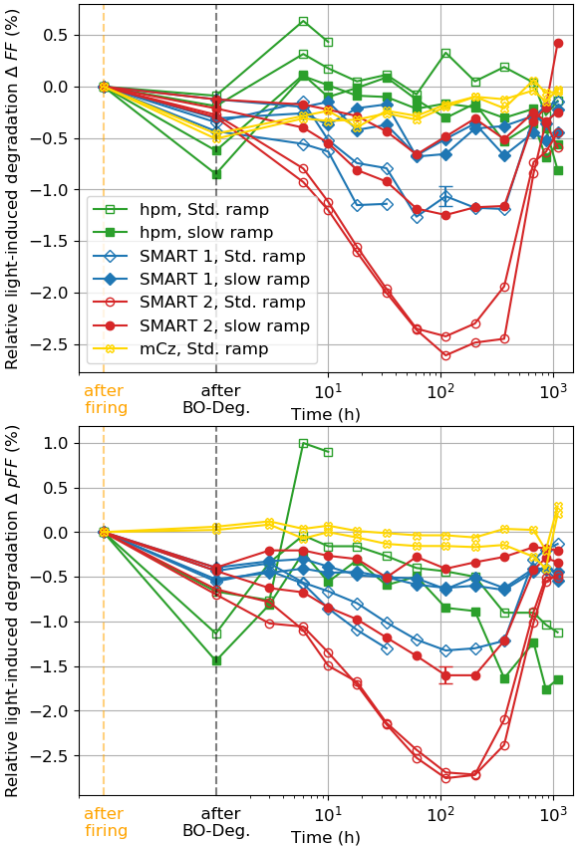

Figure 5: Relative change in FF and pFF after BO-degradation and during the LeTID test under an illumination intensity of 0.15 suns at 75 °C in reference to the respective initial value after firing. The error bars are handled as in Figure 3.

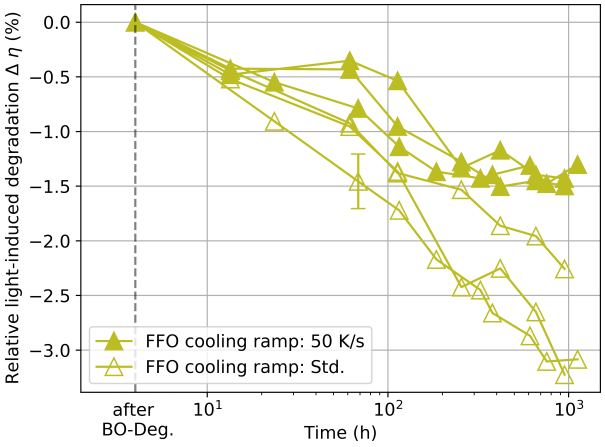

Figure 6: Relative change in η during the LeTID test under an illumination intensity of 0.15 suns at 75 °C in reference to the state after BO-degradation. The error bars are handled as in Figure 3.

3.3 IQE measurements

In Figure 7, the wavelength-dependent IQE and reflectance of two SMART 1 cells are compared for three different states in the LeTID degradation cycle. The first is the initial measurement, the second measurement was taken at the point of highest degradation (after 202 hours) and the last at the end of the LeTID test (after 1100 hours). Note that the sample in the upper graph was fired with the standard firing ramp, whereas the other one was fired with the slow ramp.

The reflectance of both samples changed very little during the LeTID test. The same is true for the IQE of the sample fired with the slow cooling ramp. For the sample fired with the standard ramp, however, the IQE measured after 202 hours of LeTID testing is reduced. While the reduction is observable from 500 nm to 1100 nm, it its most pronounced between 800 nm and 1050 nm. After 1100 hours of LeTID testing, the IQE in this regime is again very similar to that of the initial measurement. It is noteworthy that in the regime between 280 nm and 380 nm, the IQE of the initial measurement is unexpectedly high and not reached again in the subsequent measurements. This deviation can be attributed to an accidental misalignment of the xenon light source that is used at wavelengths below 400 nm.

The hpm cells also show a reduction in IQE in the wavelength spectrum from 500 nm to 1100 nm after 1100 hours (not shown here). The reduction is more pronounced in the cells fired with the standard firing ramp. Because of the limited test period, however, a regeneration phase could not be observed.

4 Discussion

4.1 Initial efficiencies

The initial efficiency data in Figure 2 shows that using a standard PERC process, SMART material is clearly superior to hpm material and is similar to mCz silicon. Since the seed-plate-related grain boundaries, which have been located intentionally within the wafer, show some recombination and industrial bricks would be cut along the defects resulting in virtually defect-free wafers, the efficiency could be further improved, narrowing or closing the efficiency gap between SMART and mCz. Further improvement of the SMART cells' efficiency is expected by optimizing the screen layout for screen printing for the exact wafer format.

The fact that the initial efficiency between cells fired with the standard-

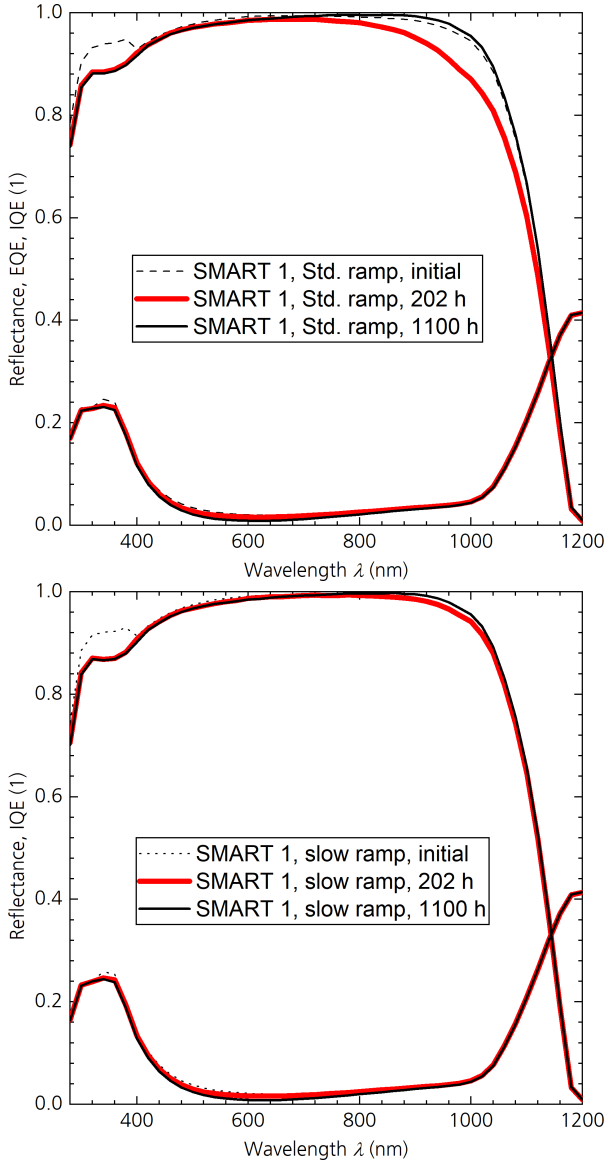

Figure 7: IQE and reflectance measurements at different wavelength of two SMART 1 cells fired with the standard (top) and the slower firing ramp (bottom) at different time points during the LeTID test

and the adapted firing profile are almost identical, probably stems from the fact, that the two profiles seen in Figure 1 are very similar to each other, especially until cooling down to 100 °C below the maximum peak temperature. We think this ensures the contact formation to be as good as in the standard process. As stated above, Figure 2 shows no significant difference in the as-processed efficiencies between standard firing and the adapted firing process.

4.2 LeTID test

In the LeTID test, the initial BO-degradation led to only a very small drop in all IV-parameters. Since all materials other than the Cz material are produced by processes which lead to very low oxygen concentrations, this was to be expected. It can also clearly be seen that the hpm and SMART cells that are fired with the standard ramp show significant LeTID behaviour. Altering the firing ramp significantly reduces the degradation in the hpm and SMART cells. The hpm cells still show LeTID degradation of $3\%_{\text{rel}}$ in η compared to $5.6\%_{\text{rel}}$ in the sample fired with the standard ramp and the trend indicates that it might have further degraded, had the test run longer. Since the degradation did not reach its maximum, we cannot exclude the possibility that in these samples the degradation reaction rate was only slowed when firing with the slow ramp. This would mean that both groups would degrade equally, only over different periods of time. We do not think this is likely to happen, and it could only possibly take place in very hot climates, as our test, as mentioned above, shows all degradation a cell would experience within 20 years in a moderate climate. If the slow ramp should however be used for the production of modules out of hpm material that will be installed in very warm climates, this possibility should be ruled out by further testing.

The fact that the degradation of the hpm cells is slower than that of the SMART cells can be explained by the lower initial V_{OC} (641 mV in comparison to 667 mV). A lower V_{OC} means a lower excess carrier density at same illumination which besides temperature is the main parameter determining the LeTID-degradation and -regeneration reaction rate [32]. When heating the wafer during the FFO process, the hydrogen diffuses from the passivation layers into the bulk. A detailed discussion of the influence of temperature on the diffusion of hydrogen trough an n-type emitter was done by Hamer *et al.* [33]. When analysing the cooling ramps, one has to consider that both diffusivity and solubility of hydrogen in silicon decreases with decreasing temperature [30, 31]. With a standard FFO profile the samples temperature and with it the diffusivity drops very quickly. The hydrogen has not enough time to react and is quenched in the bulk. With the slower cooling ramp however, the hydrogen has enough time to react to the sinking solubility and can diffuse and bind to hydrogen sinks before the diffusion rate drops so low that the hydrogen is practically immobile on the timescale of the firing process. We think this is how the slower cooling ramp mitigates LeTID. This explanation is in agreement with all recent LeTID defect models, since, as stated above, they all agree that hydrogen is somehow involved in the formation of the defect. To further understand how the slow ramp mitigates LeTID, for example what the hydrogen sinks are and where they are located, further experiments are necessary.

The mCz cells did not show any LeTID degradation, even though they were fired with a standard firing ramp. There was only a slight initial BO-degradation which slowly regenerated over the course of the test. We are not sure why the mCz material is not affected by LeTID. Should oxygen be part of the LeTID defect, one possible explanation is the low oxygen concentration of $2 \cdot 10^{17}\text{cm}^{-3}$. But since the oxygen concentration of the hpm material is similar ($1 \cdot 10^{17}\text{cm}^{-3}$ to $3 \cdot 10^{17}\text{cm}^{-3}$) this cannot be the only reason. The LeTID behaviour of the mCz will be investigated further in the future.

The Cz cells in comparison showed LeTID and the extent of it was significantly reduced by utilising the slower firing ramp. It has to be noted, however, that the BO-regeneration procedure the cells underwent before testing has been shown to influence the LeTID defect as well [34]. Moreover, the slower cooling ramp in the FFO process might affect the regenerability of the BO-defect, but we think that the trends we observe still hold. The slower degradation, compared to the SMART cells can again be partly explained by the lower initial V_{OC} (662 mV in comparison to 667 mV). Additionally, the BO-regeneration process is likely to influence the rate of LeTID degradation as well.t should also be noted that hydrogen is known to reduce the amount of BO-degradation in Cz samples [35, 36] If, as we suggested, our firing profile leads to less hydrogen in the bulk, BO-degradation might be increased in boron-doped, oxygen rich materials. Lastly, even though the cells received a BO-regeneration treatment, this only partly regenerates that defect. Because of the subsequent BO-degradation treatment, the cells are in a BO-degraded state at the beginning of the LeTID test. The BO-regeneration during testing might mask the LeTID degradation, as explained earlier. Therefore we cannot say with certainty that the reduced degradation in the cells fired with the slow FFO profile is caused by less LeTID. It is also possible that the BO-regeneration is faster in these cells. But even if this alternative

explanation were true, the new profile still showed to be beneficial to the cells.

Analysing the individual IV-parameters, J_{SC} is the dominant factor in the degradation for the hpm and the SMART 1 cells. For the SMART 2 cells the loss in FF is most influential. Comparing the degradation of SMART 1 and SMART 2 it is apparent that SMART 1 degrades more strongly in V_{OC}, while SMART 2 degrades more strongly in FF and pFF. These two effects almost completely balance each other, resulting in a only slightly stronger degradation in η of the SMART 2 cells. This behaviour can be explained with the difference in base resistivities. The SMART 1 cells with 0.8 Ωcm contain more dopant atoms than SMART 2 cells with 1.4 Ωcm, therefore the injection dependent lifetimes for the two materials are different. Since V_{OC} is measured at higher injections than pFF and FF, it is to be expected that two materials with different base doping show different amounts of degradation in these parameters.

Hammann *et al.* showed on lifetime samples that a higher base resistivity leads to less pronounced LeTID degradation [37]. This discrepancy can be explained, because only changes in V_{OC} are observable in lifetime samples. In our V_{OC} measurements, the SMART 1 cells with higher base resistivity indeed degraded more. This underlines the importance of measurements on cells to correctly determine the effect of different process parameters on LeTID degradation. It should be noted though that the difference in base resistivities analysed by Hammann *et al.* was more than 50 times larger than the difference analysed here. A comparison between the two experiments therefore has to be done with caution.

The similarity of the development of FF and pFF over time between all materials indicates that the loss in FF is due to the loss in pFF and not due to an increase of series resistance R_S. LeTID negatively affects solar cells only by increasing recombination of electrons and holes in the bulk and thereby reducing the bulk lifetime [4]. Therefore an increase in the reverse saturation current density J_0 and hence a decrease in pFF was to be expected. Moreover, the negative impact of the LeTID defect on lifetime was shown to be injection dependent [38]. The lifetime at low injections is more affected than the lifetime at high injections. This leads to a further decrease in pFF.

Because of the constant R_S, we can rule out that the reduction in efficiency during LeTID testing was caused by contact degradation. The technique of mitigating LeTID by performing an anneal with a second firing step at a temperature between 500 °C and 750 °C has shown to increase series resistance, depending on the temperature of the anneal [13, 39]. The method proposed here does not lead to this drawback.

4.3 IQE measurements

It is known that short wavelength photons up to about 500 nm are mainly absorbed in the emitter near the surface of the cell, while longer wavelength photons are mainly absorbed in the bulk [40]. The cell fired with a standard ramp shows significant losses in IQE from 500 nm to 1100 nm after illuminating with 0.15 suns on a hotplate at 75 °C for 202 h, whereas the cell with the slow cooling ramp shows no such effect. This indicates that the defect observed here was present in the bulk or rear surface of the cell, and not at the front side emitter.

As mentioned earlier, LeTID is reported to negatively affect bulk lifetime. Therefore, it was to be expected that only IQE in the range of 500 nm to 1100 nm is affected, while reflectance remains stable. Hence, the drop in IQE at the wavelengths that it was observed, confirms that the defect we analysed in this paper was indeed the bulk LeTID defect.

5 Conclusion

We have shown that the maximum amplitude of degradation within the LeTID-cycle can be effectively mitigated from $5\,\%_{rel} < \Delta\eta < 6\,\%_{rel}$ to $1\,\%_{rel} < \Delta\eta < 2\,\%_{rel}$ in hpm and SMART cells, by slightly altering the cooling ramp during the contact firing. On Cz cells that have been regenerated in an LID regeneration tool, we also showed that our method reduces the maximum amplitude of degradation by about half from $\Delta\eta \approx 3\,\%_{rel}$ to $\Delta\eta \approx 1.5\,\%_{rel}$.

The modified firing ramps do not negatively influence the initial efficiency of the cells. Unlike the case of some other LeTID mitigation techniques, no additional process steps are necessary.

The quantum efficiency analysis supports our claim that the defect we mitigated was indeed the bulk LeTID defect.

Overall, slower firing ramps seem to be a promising way to handle the LeTID challenge and ensure highest cell efficiencies throughout the entire life cycle of SMART, Cz and also hpm cells in the field.

Further research is necessary to see whether the elevated temperatures without illumination during the module lamination process impacts the LeTID stability of cells treated with this firing ramp.

Moreover, since LeTID is also present in Gallium-doped cells but seems to behave differently [41], it would be interesting to analyse whether this approach is also applicable for such cells. Using Ga-doped Cz cells would also allow to properly analyse how much Cz cells profit solely from the modified firing ramp, since a BO-regeneration step would not be necessary.

Acknowledgement

The authors acknowledge the financial support by the Federal Ministry for Economic Affairs and Energy of Germany in the project CUT-A Plus (project number 0324282). Moreover, we would like to thank Wolfram Kwapil for his remarks on the draft of this paper.

Conflict of Interest

The authors declare no conflict of interest.

References

[1] K. Kutsukake, N. Usami, Y. Ohno, Y. Tokumoto, and I. Yonenaga. Control of grain boundary propagation in mono-like si: Utilization of functional grain boundaries. *Applied Physics Express*, 6(2):025505, 2013.

[2] I. Takahashi, S. Joonwichien, T. Iwata, and N. Usami. Seed manipulation for artificially controlled defect technique in new growth method for quasi-monocrystalline si ingot based on casting. *Applied Physics Express*, 8(10):105501, 2015.

[3] S. Riepe, P. Krenckel, Y. Hayama, A. Hess, T. Trötschler, K. Kutsukake, S. Maus, F. Schindler, and N. Usami. Enhanced material quality in smart mono-si block cast ingots by introduction of functional defects. *36th European Photovoltaic Solar Energy Conference and Exhibition*, 120–125, 2019.

[4] K. Ramspeck, S. Zimmermann, H. Nagel, A. Metz, Y. Gassenbauer, B. Birkmann, and A. Seidl. Light induced degradation of rear passivated mc-si solar cells. In *27th European Photovoltaic Solar Energy Conference and Exhibition*, 861–865, 2012.

[5] F. Fertig, K. Krauß, and S. Rein. Light-induced degradation of PECVD aluminium oxide passivated silicon solar cells. *physica status solidi (RRL) - Rapid Research Letters*, 9(1):41–46, 2014.

[6] F. Fertig, I. Hoger, M. Schaper, R. Lantzsch, F. Kersten, M. Bartzsch, F. Fruhauf, B. G. Lee, A. Mette, B. Kloter, and J. W. Muller. Q.ANTUM on p-type cz silicon: high-end performance and reliability. In *2018 IEEE 7th World Conference on Photovoltaic Energy Conversion (WCPEC) (A Joint Conference of 45th IEEE PVSC, 28th PVSEC & 34th EU PVSEC)*. IEEE, 0993–0995, 2018.

[7] D. Chen, P.G. Hamer, M. Kim, T.H. Fung, G. Bourret-Sicotte, S. Liu, C.E. Chan, A. Ciesla, R. Chen, M.D. Abbott, B.J. Hallam and S.R. Wenham Hydrogen induced degradation: A possible mechanism for light- and elevated temperature- induced degradation in n-type silicon. *Solar Energy Materials and Solar Cells*, 185:174–182, 2018.

[8] J. Schmidt, D. Bredemeier, and D. C. Walter. On the defect physics behind light and elevated temperature-induced degradation (LeTID) of multicrystalline silicon solar cells. *IEEE Journal of Photovoltaics*, 9(6):14973–1503, 2019.

[9] W. Kwapil, J. Schön, T. Niewelt, and M.C. Schubert Temporary Recovery of the Defect Responsible for Light- and Elevated Temperature-Induced Degradation: Insights Into the Physical Mechanisms Behind LeTID. *IEEE Journal of Photovoltaics*, 10(6):1591–1603, 2020.

[10] D. Lin, Z. Hu, Q. He, D. Yang, L. Song, and X. Yu New insights on LeTID/BO-LID in p-type mono-crystalline silicon. *Solar Energy Materials and Solar Cells*, 226:111085, 2021.

[11] D. Chen, M. Vaqueiro Contreras, A. Ciesla, P. Hamer, B. Hallam, M. Abbott and C. Chan. Progress in the understanding of light- and elevated temperature-induced degradation in silicon solar cells: A review. *Prog. Photovolt: Res. Appl.*,1–22 2020.

[12] D. Bredemeier, D. Walter, S. Herlufsen, and J. Schmidt. Lifetime degradation and regeneration in multicrystalline silicon under illumination at elevated temperature. *AIP Advances*, 6(3):035119, 2016.

[13] C.E. Chan, D.N.R. Payne, B.J. Hallam, M.D. Abbott, T.H. Fung, A.M. Wenham, B.S. Tjahjono, and S.R. Wenham. Rapid stabilization of high-performance multicrystalline p-type silicon PERC cells. *IEEE Journal of Photovoltaics*, 6(6):1473–1479, 2016.

[14] A. Herguth, P. Keller, and N. Mundhaas. Influence of temperature on light induced phenomena in multicrystalline silicon. *AIP Conference Proceedings*, 1999(1):13007, 2018.

[15] K. Nakayashiki, J. Hofstetter, A.E. Morishige, T.A. Li, D.B. Needleman, M.A. Jensen, and T. Buonassisi. Engineering solutions and root-cause analysis for light-induced degradation in p-type multicrystalline silicon PERC modules. *IEEE Journal of Photovoltaics*, 6(4):860–868, 2016.

[16] C. Sen, C. Chan, P. Hamer, M. Wright, U. Varshney, S. Liu, D. Chen, A. Samadi, A. Ciesla, C.M. Chong, B. Hallam, and M. Abbott. Annealing prior to contact firing: A potential new approach to suppress LeTID. *Solar Energy Materials and Solar Cells*, 200:109938, 2019.

[17] P. Engelhart and F. Kersten. German patent 102013113108(a1), 2015.

[18] R. Eberle, W. Kwapil, F. Schindler, M. C. Schubert, and S. W. Glunz. Impact of the firing temperature profile on light induced degradation of multicrystalline silicon. *physica status solidi (RRL) – Rapid Research Letters*, 10(12):861–865, 2016.

[19] R. Sharma, A. G. Aberle, and J. B. Li. Optimization of belt furnace anneal to reduce light and elevated temperature induced degradation of effective carrier lifetime of p-type multicrystalline silicon wafers. *Solar RRL*, 2(9):1800070, 2018.

[20] H. Sio, H. Wang, Q. Wang, C. Sun, W. Chen, H. Jin, and D. Macdonald. Light and elevated temperature induced degradation in p-type and n-type cast-grown multicrystalline and mono-like silicon. *Solar Energy Materials and Solar Cells*, 182:98–104, 2018.

[21] M. Kim, S. Wenham, V. Unsur, A. Ebong, and B. Hallam. Impact of rapid firing thermal processes on meta-stable defects: Preformation of the letid and the suppression of b-o defects. In *2018 IEEE 7th World Conference on Photovoltaic Energy Conversion (WCPEC) (A Joint Conference of 45th IEEE PVSC, 28th PVSEC 34th EU PVSEC)*, 0341–0346, 2018.

[22] D. Ourinson, G. Emanuel, A. Csordás, G. Dammaß, H. Müller, C. Sternkiker, F. Clement and S.W. Glunz. In-situ wafer temperature measurement during firing process via inline infrared thermograph. *AIP Conference Proceedings*, 2156:020013, 2019.

[23] F. Kersten, F. Fertig, K. Petter, B. Klöter, E. Herzog, M.B. Strobel, J. Heitmann, and J.W. Müller. System performance loss due to letid. *Energy Procedia*, 124:540 – 546, 2017. 7th International Conference on Silicon Photovoltaics, SiliconPV 2017, Freiburg, Germany.

[24] VDE-AR-E 2126-4-100, Requirements for the implementation & evaluation of a LeTID test for PV cells & modules. draft, 2020.

[25] A. Herguth, G. Schubert, M. Kaes and G. Hahn. Investigations on the Long Time Behavior of the Metastable Boron–Oxygen Complex in Crystalline Silicon. *Prog. Photovolt: Res. Appl.*, 16:135 – 140, 2008.

[26] B.J. Hallam, P.G. Hamer, S. Wang, L. Song, N. Nampalli, M.D. Abbott, C.E. Chan, D.Lu, A.M. Wenham, L. Mai, N. Borojevic, A.Li, D. Chen, M. Yong Kim, A. Azmi, and S. Wenham. Advanced Hydrogenation of Dislocation Clusters and Boron-oxygen Defects in Silicon Solar Cells. *Energy Procedia*, 77:799 – 809, 2015. 5th International Conference on Silicon Photovoltaics, SiliconPV 2015, Konstanz, Germany.

[27] S. Wilking, J. Engelhardt, S. Ebert, C. Beckh, A. Herguth, and G. Hahn. High Speed Regeneration of BO-Defects : Improving Long-Term Solar Cell Performance within Seconds. *29rd EU PVSEC*, 366–372, 2014.

[28] A.A. Brand, K. Krauß, P. Wild, S. Schörner, S. Gutscher, S. Roder, S. Rein, and J. Nekarda. Ultrafast in-line capable regeneration process for preventing light induced degradation of boron-doped p-type cz-silicon perc solar cells. *33rd EU PVSEC*, 382–387, 2017.

[29] S. Maus, F. Maischner, S. Riepe, J. Greulich, E. Lohmüller, F. Schindler, P. Saint-Cast, P. Krenckel, A. Hess, S. Lohmüller, A. Wolf, and R. Preu. Smart cast-monocrystalline p-type silicon passivated emitter and rear cells: Efficiency benchmark and bulk lifetime analysis. *Solar RRL*, 5(4):2000752, 2021.

[30] A. Van Wieringen and N. Warmoltz On the permeation of hydrogen and helium in single crystal silicon and germanium at elevated temperatures. *Physica*, 22(6):849–865, 1956.

[31] M.J. Binns, S.A. Mc Quaid R.C. Newman, and E.C. Lightowlers Hydrogen solubility in silicon and hydrogen defects present after quenching. *Semiconductor Science and Technology*, 8(10):1908–1911, 1993.

[32] W. Kwapil, T. Niewelt, and M. C. Schubert. Kinetics of carrier-induced degradation at elevated temperature in multicrystalline silicon solar cells. *Solar Energy Materials and Solar Cells*, 173:80–84, 2017. Proceedings of the 7th international conference on Crystalline Silicon Photovoltaics.

[33] P. Hamer, B. Hallam, R.S. Bonilla, P.P. Altermatt, P. Wilshaw, and S. Wenham. Modelling of hydrogen transport in silicon solar cell structures under equilibrium conditions. *Journal of Applied Physics*, 123(4):043108, 2018.

[34] H. Vahlman, S. Roder, J. Nekarda, and S. Rein. High-intensity illumination treatments against letid – intensity and temperature dependence of stability and inline feasibility. *Solar Energy Materials and Solar Cells*, 223:110978, 2021.

[35] V.V. Voronkov and R. Falster. Latent complexes of interstitial boron and oxygen dimers as a reason for degradation of silicon-based solar cells. *Journal of Applied Physics*, 107(5):053509, 2010.

[36] S. Wilking, A. Herguth, and G. Hahn. Influence of hydrogen on the regeneration of boron-oxygen related defects in crystalline silicon. *Journal of Applied Physics*, 113(19):194503, 2013.

[37] B. Hammann, J. Engelhardt, D. Sperber, A. Herguth, and G. Hahn. Influencing light and elevated temperature induced degradation and surface-related degradation kinetics in float-zone silicon by varying the initial sample state. *IEEE Journal of Photovoltaics*, 10(1):85–93, 2020.

[38] F. Kersten, P. Engelhart, H. C. Ploigt, A. Stekolnikov, T. Lindner, F. Stenzel, M. Bartzsch, A. Szpeth, K. Petter, J. Heitmann, and J. W. Müller. A new mc-si degradation effect called letid. In *2015 IEEE 42nd Photovoltaic Specialist Conference (PVSC)*, 1–5, 2015.

[39] A. Peral, A. Dastgheib-Shirazi, V. Fano, J. C. Jimeno, G. Hahn, and C. del Cañizo. Impact of extended contact cofiring on multicrystalline silicon solar cell parameters. *IEEE Journal of Photovoltaics*, 7(1):91–96, 2017.

[40] S. M. Sze, Y. Li, and K. K. Ng. *Physics of semiconductor devices*, chapter 14, 800–805. John wiley & sons, 2 edition, 1981.

[41] W. Kwapil, J. Dalke, R. Post, and T. Niewelt. Influence of dopant elements on degradation phenomena in b- and ga-doped czochralski-grown silicon. *Solar RRL*.